THE JOURNAL OF BIOLOGICAL CHEMISTRY VOL. 284, NO. 31, pp. 20540–20547, July 31, 2009

Transcriptional Regulation of the Novel Toll-like Receptor *Tlr13*[*]

Received for publication, February 17, 2009, and in revised form, May 18, 2009 Published, JBC Papers in Press, June 1, 2009, DOI 10.1074/jbc.M109.022541

Zhongcheng Shi[‡§], Zhenyu Cai[‡], Shu Wen[¶], Caoyi Chen[‖], Christi Gendron[‡], Amir Sanchez[‡], Kevin Patterson[‡], Songbin Fu[§], Jianhua Yang[**], Derek Wildman[‖], Richard H. Finnell[¶], and Dekai Zhang[‡1]

From the [‡]Center for Infectious and Inflammatory Disease and [¶]Center for Environmental and Genetic Medicine at the Institute of Bioscience and Technology, Texas A&M University Health Science Center, Houston, Texas 77030, the [‖]Department of Molecular Medicine and Genetics, Wayne State University, Detroit, Michigan 48201, the [§]Laboratory of Medical Genetics, Harbin Medical University, Harbin 150081, China, and the [**]Department of Pediatrics, Baylor College of Medicine, Houston, Texas 77030

Little has been known about *Tlr13* (Toll-like receptor 13), a novel member of the Toll-like receptor family. To elucidate the molecular basis of murine *Tlr13* gene expression, the activity of the *Tlr13* gene promoter was characterized. Reporter gene analysis and electrophoretic mobility shift assays demonstrated that *Tlr13* gene transcription was regulated through three *cis*-acting elements that interacted with the Ets2, Sp1, and PU.1 transcription factors. Furthermore, our work suggests that these transcription factors may cooperate, culminating in maximal transcription of the *Tlr13* gene. In contrast, NF-κB appeared to act as an inhibitor of *Tlr13* transcription. Overexpression of Ets2 caused a strong increase in the transcriptional activity of the *Tlr13* promoter; however, overexpression of NF-κB p65 dramatically inhibited it. Additionally, interferon-β is capable of acting *Tlr13* transcription, but the activated signaling of lipopolysaccharide/TLR4 and peptidoglycan/TLR2 strongly inhibited the *Tlr13* gene promoter. Thus, these findings reveal the mechanism of *Tlr13* gene regulation, thereby providing insight into the function of *Tlr13* in the immune response to pathogen.

Upon infection, microorganisms are first recognized by cells of the host innate immune system, such as macrophages and dendritic cells, as well as mucosal epithelial cells (1–6). Recognition of pathogens is primarily mediated by a set of germ line-encoded molecules on innate immune cells that are referred to as pattern recognition receptors (7, 8). These pattern recognition receptors are expressed as either membrane-bound or soluble proteins that recognize invariant molecular structures from the pathogen called pathogen-associated molecular patterns (7, 8).

Recent studies on the recognition of microbial pathogen-associated molecular patterns have highlighted the vital role of one group of pattern recognition receptors, the Toll-like receptors (TLRs)[2] (9, 10). It is already clear that TLRs play a crucial role in the recognition of "molecular signatures" produced by infecting microbes to engage differential signaling pathways (11, 12). Signaling through TLRs activates various transcription factors, such as nuclear factor-κB (NF-κB), activating protein-1 (AP-1), and interferon regulatory factors to induce an immunological response (3, 11).

Tlr13 is a novel and poorly characterized member of the Toll-like receptor family (3, 13). Although the elucidation of the function of *Tlr13* depends mainly on the identification of its natural ligand, its transcriptional regulation also provide some clues. For example, which type of cells expresses *Tlr13*? Which transcription factors control *Tlr13* expression? How do different pathogen-associated molecular patterns from different pathogens regulate *Tlr13* expression? This information will perhaps help us understand not only how this novel TLR responds to different infections but also which pathogens might be recognized by *Tlr13* to activate the innate immune response. Recently, Aderem *et al.* (14) reported that *Tlr13* belongs to the *Tlr11* subfamily based on phylogenic analysis. We previously demonstrated that *Tlr11* primarily expresses on epithelial cells and recognizes urinary pathogenic *Escherichia coli* (15) and profillin-like protein from parasite (16). We therefore studied transcriptional regulation of *Tlr13* upon stimulation mainly with bacterial components, the results of which can be used as the starting point for characterization of this novel TLR.

EXPERIMENTAL PROCEDURES

Cell Lines and Reagents—RAW 264.7, NIH 3T3, and HEK 293 cells were purchased from ATCC. These cells were cultured in Dulbecco's modified Eagle's medium (Invitrogen) and supplemented with 10% (v/v) heat-inactivated fetal bovine serum (HyClone), 100 units/ml penicillin, and 100 μg/ml streptomycin at 37 °C in a 5% CO_2 incubator. All of the TLR ligands were purchased from Invivogen. Antibodies for supershift analyses were purchased from Santa Cruz Biotechnology, Inc. (Santa Cruz, CA). Bacteria used in this study, including the *Staphylococcus aureus* K2 strain and the urinary pathogenic *E. coli* 8NU strain (15), were frozen at −80 °C in 1-ml aliquots in 10% glycerol at 2×10^8 colony-forming units/ml. The frozen aliquots were thawed and heat-killed before each use. Recombinant mouse IFN-β was purchased from R&D Systems.

Isolation of Total RNA and RT-PCR—Total RNA was isolated with TRIzol reagent (Invitrogen). cDNA was prepared by oligo$(dT)_{12-18}$ and reverse transcriptase SuperScript II from Invitrogen with 2 μg of DNase I-treated total RNA. One μl of cDNA was amplified using the primers shown in Table 1. The parameters of the PCR were as follows: denaturation at 94 °C

* This work was supported, in whole or in part, by National Institutes of Health Grant AI072263. This work was also supported by the Texas A&M University Health Science Center.

[1] To whom correspondence should be addressed: 2121 W. Holcombe Blvd., Houston, TX 77030. Fax: 713-677-7576; E-mail: dzhang@ibt.tamhsc.edu.

[2] The abbreviations used are: TLR, Toll-like receptor; EMSA, electrophoretic mobility shift assay; MEK, mitogen-activated protein kinase/extracellular signal-regulated kinase kinase; RACE, rapid amplification of cDNA ends; RT, reverse transcription; PGN, peptidoglycan; LPS, lipopolysaccharide; ERK, extracellular signal-regulated kinase; IFN, interferon.

TABLE 1
Sequences of oligonucleotides used in EMSA, site-directed mutagenesis, and RT-PCR
The underlined letters indicate mutated nucleotides.

Oligonucleotide	Sequence (5′ → 3′)	Purpose
TLR13R369	GCGGCAGAGAAAATCCTACTAAC	5′-RACE-PCR
TLR13R299	GACTGTCTTAGGCATCCAGGTTAC	5′-RACE-PCR
NF-κB wild type	ATCTGGCTGAGCATCCCCAAATGAGCCTA	EMSA/mutagenesis
NF-κB mutant	ATCTGGCTGAGCAGCCACAAATGAGCCTA	EMSA/mutagenesis
Ets2 wild type	GAGAAGAGGAAGGAAATGTCTCATGTCC	EMSA/mutagenesis
Ets2 mutant	GAGAAGAGGTTCATAATGTCTCATGTCC	EMSA/mutagenesis
Sp1mF	GGCCAGGTACGTTGCAGGATGGTTTC	Mutagenesis
Sp1mR	GCAAACCATCCTGCAACGTACCTGGC	Mutagenesis
PU.1mF	TCTTTTGGAACTTCATAAGGAAATGTCTCA	Mutagenesis
PU.1mR	TATGAAGTTCCAAAAGATTTAGGCATGGCG	Mutagenesis
TLR13F	TGTCTGCTCTGGTGGACTTG	RT-PCR
TLR13R	GAGGAGTGAAGGCGTCTTTG	RT-PCR
β-actin-F	AATCCTGTGGCATCCATGAAAC	RT-PCR
β-actin-R	AACGCAGCTCAGTAACAGTCCG	RT-PCR
Ets2-B-F	CCAGGATCCATGAATGACTTTGGAATCAAG	Cloning
Ets2-E-R	GGAGAATTCGAGTCTTCTGTATCAGGCTGG	Cloning
PU.1-B-F	CCAGGATCCATGTTACAGGCGTGCAAAATG	Cloning
PU.1-E-F	GGTGAATTCGTGGGGCGGGAGGCGCCGCTC	Cloning
Sp1-H-F	GGAAGCTTATGAGCGACCAAGATCACTC	Cloning
Sp1-E-R	GGGAATTCCCGAAACCATTGCCACTGATAT	Cloning
Raf1-B-F	GGAGAATTC ATGGAGCACATACAGGGAGC	Cloning
Raf1-E-R	GGAATTCCCGAAGACTGGTAGCCTTGG	Cloning

for 3 min followed by 25–35 cycles of 94 °C for 20 s, 57 °C for 20 s, and 72 °C for 30 s. The PCR products were subjected to electrophoresis in 1.5% agarose gels, visualized under UV light after ethidium bromide staining, and then imaged.

RNA Ligase-mediated 5′-RACE-PCR—To determine the transcription start site, we performed 5′-RACE-PCR using the First Choice RLM-RACE Kit (Ambion). RAW 264.7 RNA was first treated with calf intestinal phosphatase to remove free 5′-phosphates from all RNA molecules. The RNA was then treated with tobacco acid pyrophosphatase to remove the cap structure, leaving a 5′-monophosphate. A 45-base RNA adapter oligonucleotide was ligated to 10 μg of the treated RNA using T4 RNA ligase. A random-primed reverse transcription reaction was performed using Moloney murine leukemia virus reverse transcriptase and then followed by nested PCR to amplify the 5′-end of murine TLR13. The gene-specific primers are listed in Table 1. The PCR product was cloned into pJET1.2/blunt Cloning Vector (Fermentas) and sequenced.

Plasmid Constructions—Mouse cDNA encoding full-length Ets2, Sp1, PU.1, and Raf were PCR-amplified from a mouse spleen cDNA library using the primers shown in Table 1. All PCR products were gel-purified (Qiagen) and cloned into the mammalian expression vector pcDNA3.1/V5/Myc (Invitrogen). The PCR products were verified by sequencing and then further confirmed by immunoblotting using an anti-Myc antibody purchased from Invitrogen. Mouse NF-κB p65 expression plasmid was a gift from Dr. S. Ghosh (Yale University).

Cloning and Sequencing of the 5′-Flanking Region of the Tlr13 Gene—Murine genomic DNA (C57/B6 strain) was amplified with the Expand High Fidelity PCR system (Roche Applied Science) according to the manufacturer's instructions. PCR conditions were as follows: 92 °C for 2 min, one cycle; 92 °C for 15 s, 57 °C for 20 s, and 68 °C for 2 min for 30 cycles; and one cycle of incubation at 68 °C for 5 min. Murine *Tlr13*-specific amplification was achieved using the sense primer 5′-GTGGTACCACAGTTCCACTAACTG-3′, containing a KpnI restriction enzyme site, and the antisense primer 5′-GCAGATCTGCTAAACAATGACATTCTG-3′, containing a BglII restriction enzyme site. An approximately 1.9-kb fragment that contains the immediate 5′-flanking *Tlr13* sequence of the putative murine *Tlr13* promoter (GenBank™ number EU588988) was obtained. This 1.9-kb KpnI/BglII fragment was subcloned into the pGL3 basic vector (Promega). The complete sequence was determined with autosequencing by the Protein and Nucleic Acid Chemistry Facility at Baylor College of Medicine in Houston. Truncated mutants of the 5′-flanking region were also cloned into the pGL3 with the same restriction enzyme sites. Mutations and deletions of putative transcription factor binding sites were carried out by two-step PCR mutagenesis with the primers listed in Table 1.

Transient Transfections and Luciferase Assay—All transfections were performed in triplicate in 24-well plates. Approximately 2×10^5 cells/well were seeded 24 h before transfection. Following the manufacturer's instructions, plasmids were transfected into cells using Lipofectamine 2000 (Invitrogen). Briefly, 0.8 μg of reporter plasmids together with 0.02 μg of *Renilla* pRL-TK vector (Promega) were diluted with Opti-MEM and then mixed with diluted Lipofectamine 2000. After a 20-min incubation at room temperature, the mixtures were added to each well. At 24 h post-transfection, cells were either analyzed for luciferase activity or further challenged with different agonists of TLRs for the treatment times indicated. Luciferase assays were performed using the Dual Luciferase Assay System (Promega), which contains an internal control that is detectable simultaneously with the luciferase reporter gene. Each experiment was conducted a minimum of three times.

Nuclear Extract Preparation and Electrophoretic Mobility Shift Assay (EMSA)—Nuclear extracts of RAW 264.7 cells were prepared as described previously (17). Briefly, RAW 264.7 cells were harvested by scraping in phosphate-buffered saline, pelleted, and then lysed in 500 μl of lysis buffer containing 0.5% Nonidet P-40, 10 mM HEPES, 10 mM KCl, 1.5 mM $MgCl_2$, 0.5 mM dithiothreitol, and protease inhibitor mixture (Roche Applied Science). Intact nuclei were pelleted by centrifugation at 12,000 × *g* at 4 °C for 5 min and lysed in 150 μl of nuclear lysis buffer containing 20 mM HEPES (pH 7.5), 25% glycerol, 0.42 M NaCl, 0.2 mM EDTA, and protease inhibitor mixture. The protein concentration was determined using the BCA assay (Pierce). The double-stranded DNA probes used in the gel mobility shift assays are shown in Table 1. The EMSA was performed using Gel Shift Assay Systems (Promega). Briefly, 2.5 μg of nuclear extract was incubated with 10 ng of each labeled probe in binding buffer containing 0.5 mM EDTA, 0.5 mM dithiothreitol, 4% glycerol, 1 mM $MgCl_2$, 50 mM NaCl, 10 mM Tris-HCl (pH 7.5), and 0.05 mg/ml poly(dI-dC)-poly(dI-dC) for 20 min at room temperature. To demonstrate sequence-specific binding, some of the reactions contained a 100-fold excess of the same unlabeled probe and other unlabeled probes to determine specific and nonspecific binding. Furthermore, specific antibodies against p65 and p50 for supershift assays were included in other reactions. The reaction mixtures were then separated in a 6% non-denaturing polyacrylamide gel at room temperature in 0.5× TBE buffer at 100 V for 3 h. The gel was transferred to Whatman 3MM paper, dried, and exposed to x-ray film overnight at −70 °C with an intensifying screen. The

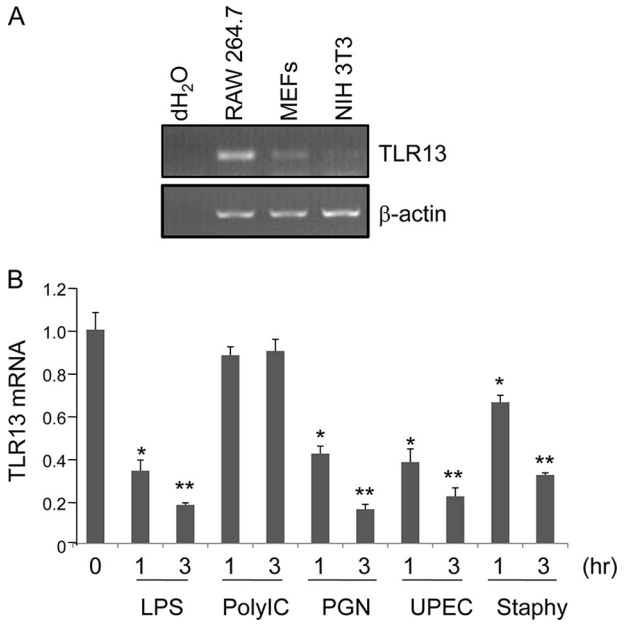

FIGURE 1. **Suppression of *Tlr13* mRNA expression by LPS, PGN, and bacterial lysates in macrophage RAW 264.7 cells.** *A*, regular RT-PCR was performed to analyze *Tlr13* and β-actin mRNA expression in various murine cell lines, including RAW 264.7 cells, mouse embryonic fibroblasts, and NIH 3T3. *B*, real time PCR analysis was performed to quantitate *Tlr13* expression in RAW 264.7 cells treated with 40 μl/ml bacterial lysates, 5 μg/ml PGN, 100 ng/ml LPS, or 25 μg/ml poly(I-C) for 1 or 3 h, as indicated. *Staphy*, Gram-positive *Staphylococcus aureus* K2 strain; *UPEC*, Gram-negative urinary pathogenic *E. coli* 8NU strain. The *graph* shows the mean ± S.D. of three independent experiments; *, $p < 0.05$; **, $p < 0.001$. Statistical analysis was performed by Student's *t* test.

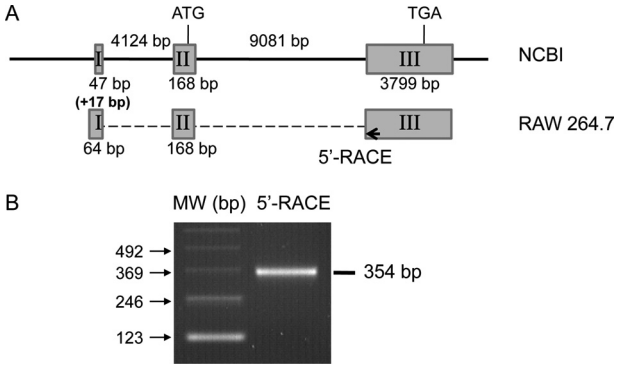

FIGURE 2. **Structure of murine *Tlr13* gene and determination of the *Tlr13* transcription start site.** *A*, physical map of the murine *Tlr13* gene and the strategy of 5′-RACE PCR amplification are shown. *Tlr13* has three exons; the transcriptional start site was mapped by 5′-RACE PCR. The oligonucleotide location used for 5′-RACE PCR was indicated by an *arrow*, and the size of the 211-bp PCR product was determined after sequencing. Exon I in Raw264.7 cells is 17 bp longer than it is in the NCBI data base (GenBank™ number EU588988). *B*, 5′-RACE PCR product was resolved on a 2% agarose gel with only one specific band. The determined transcription start site is based on the specific PCR product after sequencing.

probes used for EMSA are listed in Table 1. Supershift analyses were performed as described (18).

Quantitative RT-PCR—Total RNA was isolated from cells using the RNAeasy kit (Qiagen). For each sample, 1 μg of total RNA was reverse transcribed using Superscript II reverse transcriptase (Invitrogen). The reverse transcription reaction was diluted 1:10, and 2 μl of the diluted sample was added to an 18-μl PCR assay mixture containing a 0.5 μM concentration of each primer and 1× SYBR Green JumpStart Taq ReadyMix (Sigma). PCR was conducted with the MyiQ single-color real time PCR detection system (Bio-Rad) using the following conditions: hot start activation at 95 °C for 10 min followed by 40 cycles of 95 °C for 15 s, 61 °C for 30 s, and 72 °C for 30 s. Two sets of PCR assays were performed for each sample using the primers listed in Table 1. The threshold cycle number for *Tlr13* was normalized to that of β-actin, and the resulting value was converted to a linear scale. All assays were performed at least three times from independent RNA preparations.

RESULTS

Characterization of Tlr13 Gene Expression in Macrophage RAW 264.7 Cells—Tlr13 is a novel member of the mammalian Toll-like receptor family, and little is known about its expression and function (3, 13). We therefore started by analyzing *Tlr13* gene expression in various murine cell lines, including RAW 264.7 macrophages, mouse embryonic fibroblasts, and NIH 3T3 fibroblasts by semiquantitative RT-PCR. As shown in Fig. 1*A*, RAW 264.7 cells constitutively expressed the highest level of mRNA for *Tlr13* among the cell types tested. We then pursued the transcriptional responses of *Tlr13* upon stimulation in RAW 264.7 cells. *Tlr13* mRNA levels were monitored by real time RT-PCR after incubation of RAW 264.7 cells with various TLR agonists, including 5 μg/ml peptidoglycan (PGN), 100 ng/ml LPS, and 25 μg/ml poly(I-C) (mimic of viral double-stranded RNA), as well as Gram-positive (*S. aureus* K2 strain) and Gram-negative (urinary pathogenic *E. coli* 8NU strain) bacterial lysates. Surprisingly, as shown in Fig. 1*B*, we found that the expression of *Tlr13* with various treatments was significantly reduced 1 h after treatment; levels subsequently declined over longer time periods (Fig. 1*B*). Specifically, at 3 h post-treatment, the original level of *Tlr13* mRNA was reduced by more than 80% by heat-killed bacteria and reduced by about 60–90% by PGN and LPS, respectively. In contrast, poly(I-C) treatment did not overly alter *Tlr13* expression levels (Fig. 1*B*).

Determination of the Transcription Start Site of the Murine Tlr13 Gene—To facilitate the cloning of the *Tlr13* promoter constructs, the transcription initiation site of the mouse *Tlr13* gene was determined by RNA ligase-mediated rapid amplification of cDNA 5′-ends (RLM-RACE) PCR using mRNA isolated from murine macrophage RAW 264.7 cells, which strongly express *Tlr13* mRNA (Fig. 1*A*). The reverse primer was oligonucleotides that were complementary to the nucleotide position 299 bp downstream of the reported *Tlr13* mRNA sequence (GenBank™ number NM_205820). The gene structure and the strategy designed for the 5′-RACE PCR are shown in Fig. 2*A*. After RLM-RACE PCR, only one specific 354-bp product was obtained (Fig. 2*B*). This PCR product was then cloned and sequenced. We discovered that the exon I in Raw264.7 cells is 17 bp longer than it is in the NCBI data base (Fig. 2*A*; GenBank™ number EU588988). The sole transcription start site was found 196 bp upstream of the first adenine residue within the start codon (Fig. 2*A*). The mRNA transcription initiation site is designated as +1 in the numbering of the nucleotide sequence throughout this study.

Cloning and Sequencing of the Murine Tlr13 Promoter—Based on the determined location of the transcriptional start site, we next analyzed the *Tlr13* 5′-flanking region for a func-

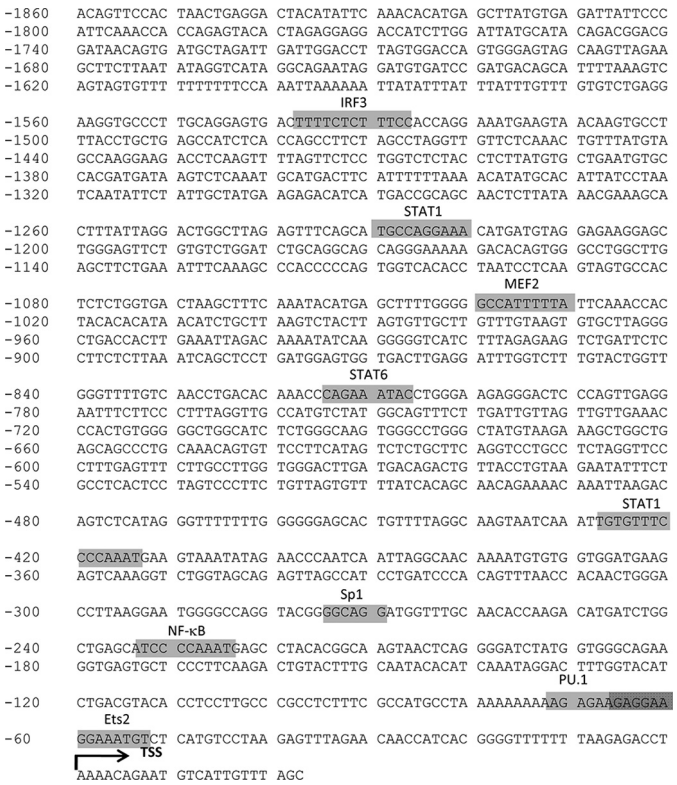

FIGURE 3. **Sequence of the 5′-flanking region of the murine *Tlr13* gene.** Shown is a 1.9-kb sequence of the 5′-flanking region of murine *Tlr13*. *Underlined* sequences are the potential transcription factor binding sites predicted by MatInspector software. The *arrow* indicates the transcription start site (*TSS*), which was determined by 5′-RACE.

tional promoter using MatInspector, a promoter analysis software (19). We obtained *Tlr13* promoter sequence from murine chromosome X genomic contig (GenBank NT_039706), and cloned an approximately 1900-bp fragment, a region spanning 1860 bp upstream and 23 bp downstream of the transcriptional start site. Nucleotide sequence analysis of the 5′-flanking region of the murine *Tlr13* gene (GenBank™ number EU588988) revealed the absence of a canonical TATA box (Fig. 3). We identified several potential DNA-binding motifs in the promoter region, including NF-κB, Sp1, PU.1, and Est2 sites (Figs. 3 and 4*A*).

Identification of cis-Acting Elements within the Tlr13 Gene Promoter—Progressive 5′ deletions of *Tlr13* gene promoter constructs were generated to determine DNA transcription regulatory elements. Mouse macrophage cell line RAW 264.7 cells, mouse embryonic fibroblasts, and HEK 293 cells were transfected with the *Tlr13* plasmid DNA constructs as well as the pRL-TK vector as an internal control for normalizing transfection efficiency. Serial 5′-deletion mutations of the full-length promoter revealed a pattern of functional activity in transfected cells (Fig. 4*A* and supplemental Fig. 1). The highest level of luciferase activity was associated with the −341 fragments. Fragments larger than −1380 bp resulted in less luciferase activity, suggesting that the region from −1380 to −1000 bp contained negative regulatory elements. In contrast, deletions from −341 to −258 bp led to a remarkable reduction of the activity in RAW 264.7 cells (Fig. 3*A*) as well as in 293 cells and mouse embryonic fibroblasts (supplemental Fig. 1), indicating that this 83-bp region contained functional and essential transcription elements that drive maximal promoter activity. The region within −341 bp of the *Tlr13* promoter contains multiple possible transcription factor binding sites, including NF-κB, Sp1, PU.1, and Est2 sites (Figs. 3 and 4*A*).

To pinpoint the functional significance of the NF-κB, Sp1, PU.1, and Est2 binding sites detected within the *Tlr13* promoter, we used site-directed mutagenesis to mutate each of these sites and then assayed their effects on luciferase activity in RAW 264.7 cells (Fig. 4*B*). Disruption of the Sp1 site dramatically impaired the p-341 promoter's activity by ~70%. Furthermore, deletion of either Ets2 or PU.1 binding sites completely abolished its activity. In contrast, mutation of the NF-κB binding site, which plays an important role in the transcriptional regulation of most other TLRs, did not affect *Tlr13* promoter activity (Fig. 4*B*). We observed that p65 overexpression can also inhibit the NF-κB- mutated *Tlr13* promoter (Fig. 4*B*), indicating that the inhibition of *Tlr13* expression by p65 is independent of the NF-κB binding site within the *Tlr13* promoter. Thus, Sp1, PU.1, and Ets2 elements act as essential *cis*-acting elements within the *TLR13* promoter, because they are necessary to reach maximal transcriptional activity.

Suppression of the Murine Tlr13 Gene Promoter by LPS and PGN but Not by Poly(I-C)—To determine the molecular mechanisms underlying LPS-, PGN-, Gram-positive bacterial lysate-, and Gram-negative bacterial lysate-mediated decrease in *Tlr13* mRNA (Fig. 1*B*), the effects of LPS, PGN, and other compounds on *Tlr13* gene promoter activity were examined using macrophage RAW 264.7 cells transfected with the *Tlr13* promoter construct p-341. The p-341 construct was chosen for these studies, because it showed the highest activity. After the cells were treated with LPS or PGN, luciferase activity levels were significantly decreased. In contrast, poly(I-C) treatment did not dramatically alter the promoter's activity, whereas the treatment with IFN-β significantly increased it (Fig. 5*A*). Furthermore, PS1145 (an IKK inhibitor) did abolish the capacity of LPS-mediated *Tlr13* down-regulation (Fig. 5, *B* and *C*), indicating that NF-κB was involved in this down-regulation.

Identification of Transcription Factors That Interact with the Essential cis-Acting Elements—To elucidate potential transcription factors that interact directly with the identified *cis*-acting elements of *Tlr13*, a gel EMSA was performed. Oligonucleotides corresponding to the binding sites from NF-κB, PU.1, Ets2, and Sp1 in the *Tlr13* promoter were designed for these experiments. The mobility of each labeled DNA probe was altered in the presence of nuclear protein prepared from RAW 264.7 cells (Fig. 6); a weak, but positive binding signal was detected in the case of NF-κB and Sp1 (data not shown). The binding specificity of each probe was verified using anti-Ets2 antibody, in the case of Ets2, or the addition of excessive unlabeled oligonucleotide competitor, in the case of PU.1. Interestingly, NF-κB p65 overexpression is capable of inhibiting Ets2 binding in a dose-dependent manner (Fig. 6*C*).

Characterization of the trans-Activators of the Tlr13 Promoter—To further investigate the role of potential *trans*-activators (including Ets2, PU.1, and Sp1) in transcriptional regulation of the *Tlr13* gene, we co-transfected the p-341 *Tlr13* promoter with Ets2, PU.1, and Sp1 expression vectors of into

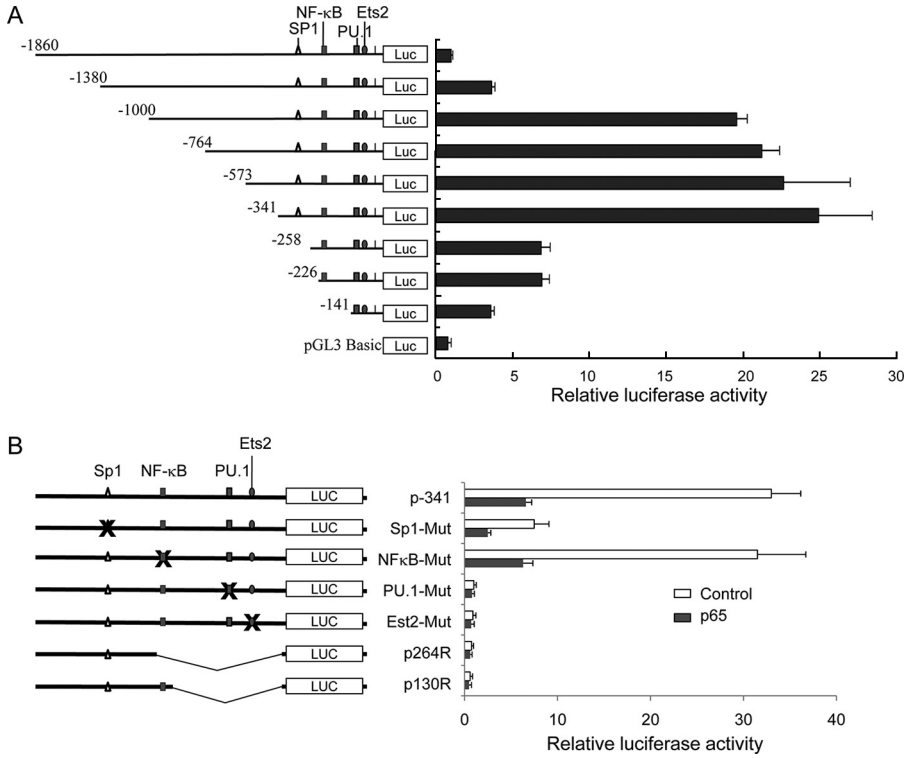

FIGURE 4. **Identification of essential *cis*-acting elements within the *Tlr13* promoter.** *A*, deletion analysis of the *Tlr13* gene promoter. The truncated promoter fragments with luciferase reporter gene constructs (*Luc*) were contransfected with the *Renilla*-TK luciferase vector into RAW 264.7 cells. Firefly luciferase activity is relative to the *Renilla*-TK luciferase activity; values are the means ± S.D. obtained from three independent experiments. Deletions from −341 to −258 bp led to an extreme reduction of the activity. The region within −341 bp of the *Tlr13* promoter contains multiple potential important transcription factor binding sites, including NF-κB, Sp1, and Est2. *B*, site-directed mutation analysis of the *Tlr13* gene promoter. RAW 264.7 cells were transiently transfected with p65 expression vector or control vector plus the p-341 promoter plasmid or the constructs with different mutations of the Sp1, NF-κB, PU.1, or Ets2 site, respectively. Transfected cells were harvested after 24 h of transfection for the luciferase assay. Firefly luciferase activity was normalized to *Renilla* luciferase activity, and the values represent the means ± S.D. of three independent experiments.

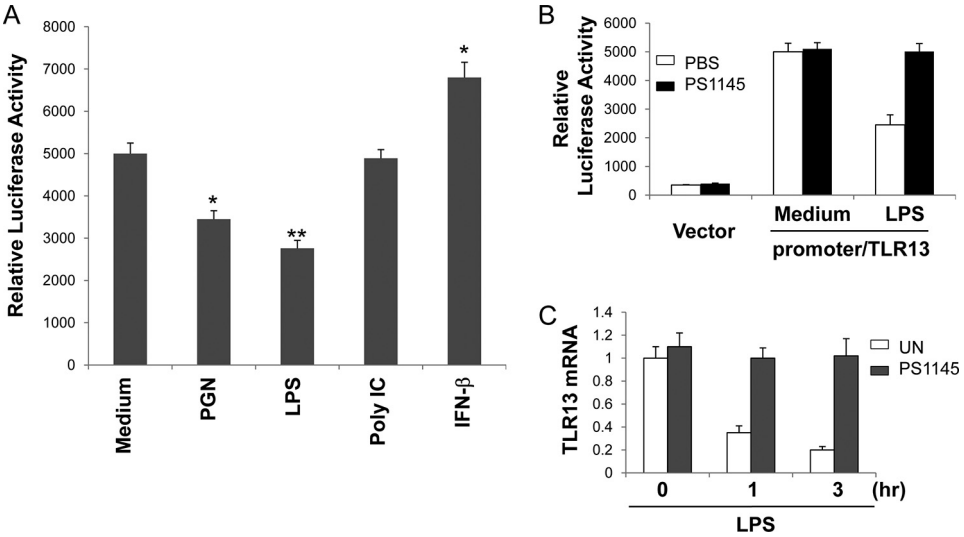

FIGURE 5. **Suppression of the *Tlr13* gene promoter by LPS and PGN.** *A*, Raw264.7 cells were transfected with *Tlr13* promoter p-341 plus *Renilla*-TK luciferase vector by Lipofectamine 2000. Twenty-four hours after transfection, cells were treated with medium alone, 5 μg/ml PGN, 100 ng/ml LPS, 25 μg/ml poly(I-C), or 100 units/ml IFN-β. Firefly luciferase activity was assayed 6 h after treatment and normalized to *Renilla* luciferase activity. Data present the mean ± S.D. of three independent experiments. Statistical analysis was performed by Student's *t* test; *, $p < 0.05$; **, $p < 0.005$. *B*, all of the procedure was performed in the same way as in *A* except for the pretreatment with PS1145 (10 μM for 3 h) or PBS before LPS stimulation. *C*, Raw264.7 cells were pretreated with PS1145 (10 μM for 3 h) or left untreated (*UN*) and then stimulated with LPS (100 ng/ml) for 0, 1, or 3 h. The endogenous *Tlr13* expression was analyzed by real time PCR.

RAW 264.7 cells. As shown in Fig. 7*A*, overexpression of Ets2 increased the transcription activity of the *Tlr13* promoter by 15–20-fold. In contrast, overexpression of Sp1 and PU.1 failed to activate it. Instead, overexpression of PU.1 inhibited Ets2-mediated *Tlr13* promoter activity, perhaps because the overexpression of PU.1 might compete with endogenous PU.1. Since transcription factors are able to directly bind to *cis*-acting elements, we believe that the transcriptional factor Ets2 activates the *Tlr13* promoter through its binding motif. Furthermore, we also confirmed that p65 directly interacts with Ets2 after LPS stimulation (Fig. 7*B*). We explored the Ets2 role in the Ets2 wild type compared with Ets2 mutated promoter activity. Indeed, Ets2 increased the activity only in Ets2-wild type promoter but not in the Ets2 mutated promoter in a dose-dependent pattern (Fig. 7*C*). Since Ets2 activation is controlled by the Raf/MEK/ERK pathway, and overexpression of Raf is able to activate Ets2 expression (20), we overexpressed Raf to check whether it can also activate mTLR13 promoter activity in RAW 264.7 cells. As expected, Raf overexpression stimulated the *Tlr13* promoter activity and co-transfection with Ets2 and showed the apparent synergy (Fig. 7*D*).

DISCUSSION

In this study, the activity of the *Tlr13* gene promoter was characterized to elucidate the molecular basis of murine *Tlr13* gene expression. We demonstrate that Ets2, PU.1, and Sp1 sites within the *Tlr13* promoter region act as *cis*-acting elements and have a critical role in the transcriptional regulation of the *Tlr13* gene. In contrast, NF-κB acted as a suppressor. Overexpression of Ets2 and NF-κB p65 potently *trans*-activated and inhibited the *Tlr13* gene promoter, respectively. The activated signaling of LPS/TLR4 and PGN/TLR2 strongly inhibited the *Tlr13* gene promoter.

Ets2 is a member of the Ets transcription factor family that plays a

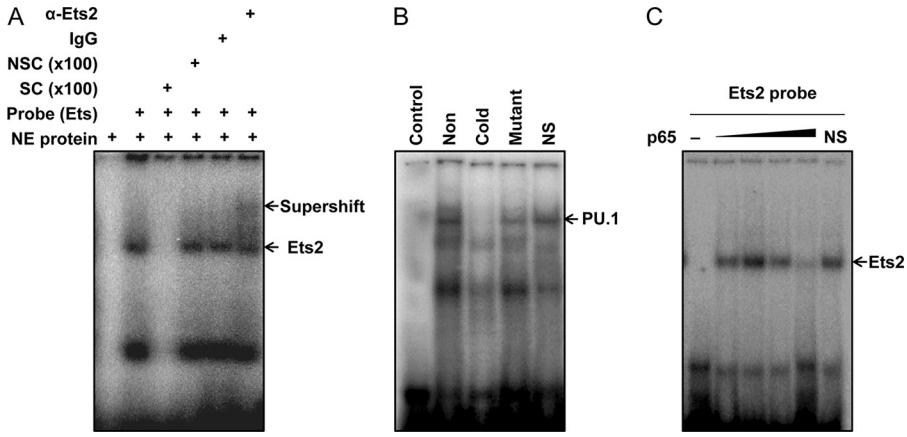

FIGURE 6. **Binding of PU.1 and Ets2 to the promoter.** Electrophoretic mobility shift assay (EMSA) targets the identified elements with potential important for transcriptional regulation in the *Tlr13* promoter, including Ets2 (*A* and *C*) and PU.1 (*B*). A radiolabeled double-stranded DNA probe containing the Ets2 (*A* and *C*) and PU.1 (*B*) binding region in the *Tlr13* promoter was incubated with nuclear extracts from RAW 264.7 cells and separated on a 6% polyacrylamide gel. Specificity was determined by the addition of antibodies for supershift, a 100-fold molar excess of unlabeled cold probe, mutant probe, or other control probe as specific and nonspecific competitors, as indicated *above* the corresponding *lanes*. The *arrowheads* indicate specific complexes with the specific element. *Control*, probe only without nuclear extracts. *C*, overexpression of NF-κB p65 is capable of inhibiting Ets2 binding in a dose-dependent manner. RAW264.7 cells were transfected with empty vector and p65 at a ratio of 99:1, 90:10, and 0:100 for *lanes 3–5*, respectively. *NS*, nonspecific.

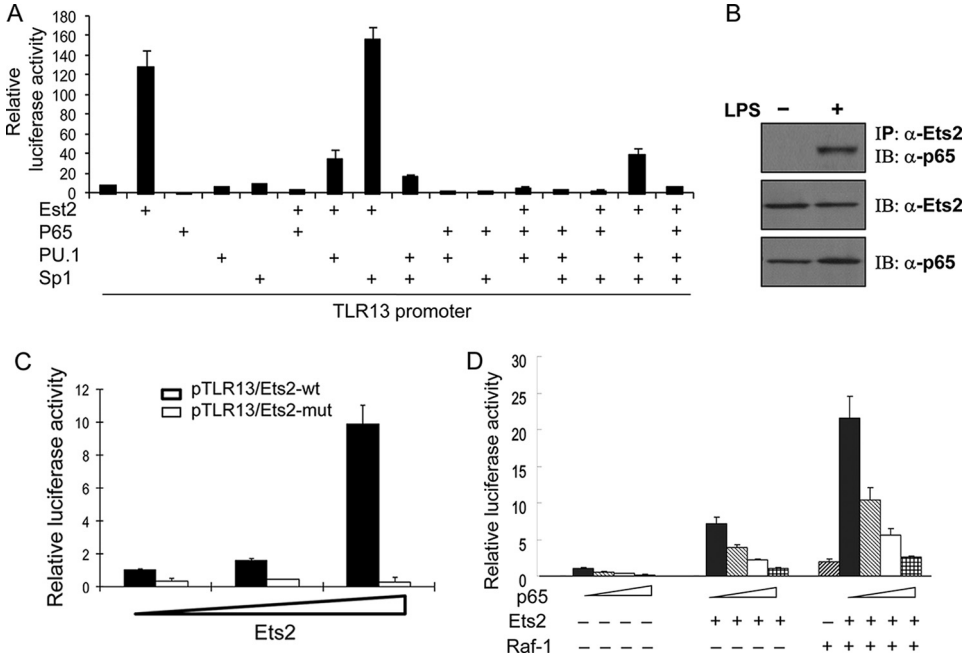

FIGURE 7. **Characterization of the transcription factors in the murine *Tlr13* gene promoter.** *A*, RAW 264.7 cells were transfected with *Tlr13* promoter p-341 plus expression vector for Ets2, p65, PU.1 and Sp1, respectively, and with different combinations of expression vectors. Transfected cells were harvested after 24 h for the luciferase assay. *B*, Raw264.7 cells were treated with LPS (100 ng/ml) for 0.5 h. Cells were lysed at 48 h post-transfection. Total protein was harvested and was used to perform immunoblotting (*IB*) and immunoprecipitation (*IP*) by the antibodies as indicated. Similar results were obtained in three independent experiments. *C*, RAW 264.7 cells were transfected with wild type p-341 or Ets2 site mutation p-341 plasmids plus different doses of Ets2 expression construct. *D*, RAW 264.7 cells were transfected with wild type p-341 or Ets2 site mutation p-341 plasmids plus expression vectors for Ets2, Raf-1, and the combination of Ets2 and Raf-1. Transfected cells were harvested after 24 h for the luciferase assay.

role in many biological processes, including cellular proliferation, differentiation, development, transformation, and apoptosis. Ets binding sites are among the eight most important DNA motifs (21). Recently, it has been shown that Ets also plays a role in the immune response (*e.g.* Ets2 regulated *TLR9* expression) (22). Here, we show that *Tlr13* might be another Ets2 target gene in the regulation of the immune response; ETS2 can significantly increase murine *Tlr13* promoter activity and strongly up-regulate endogenous *Tlr13* expression. All of the ETS members can be directly phosphorylated by the ERK molecules through the Raf/MEK/ERK pathway (20). For example, Ets2 can be phosphorylated by ERKs on Thr^{72}, which leads to Ets2 activation (23). The activated ETS2 binds to target promoters and triggers transcription of the regulated genes. ETS2 regulates the expression of several cytokines in the inflammatory reaction. In mice, Thr^{72} phosphorylation of *Ets2* is required for the persistent activation of tumor necrosis factor-α in macrophages stimulated with LPS (24). Moreover, *Ets2* can directly bind to and activate the promoters of IL-5 (25), IL-10 (26), and IL-12 (27, 28). More interestingly, Ets2 is involved in the development and differentiation of macrophages and T cells. This implies that Ets2 has a role in host defense. To exemplify, studies with *Ets2-lacZ* transgenic mouse have showed that these mice undergo abnormal macrophage development during the first 40 days after birth. Furthermore, peritoneal macrophages obtained from these transgenic animals did not exhibit the characteristic macrophage morphological features when cultivated *in vitro* with CSF-1 stimulation (29, 30).

PU.1 is also a member of the Ets family of transcription factors that is specific for macrophage and B cells (31). PU.1 regulates TLR expression; it up-regulates *TLR2* and *TLR4* (32) but down-regulates TLR9 (33). However, it is not clear how PU.1 distinctly regulates each TLR. For the *Tlr13* promoter, we found that mutating the PU.1 binding site abolished the promoter activity. In fact, the PU.1 and Ets2 binding sites are overlapping. Comparing the results of our PU.1 and Ets2 overexpression studies, we concluded that Ets2 exerted the more significant activator for *Tlr13* expression.

Tlr13 gene transcription is also regulated through another *cis*-acting element that interacts with the transcription factor Sp1. Sp1 is a ubiquitous factor that regulates the constitutive

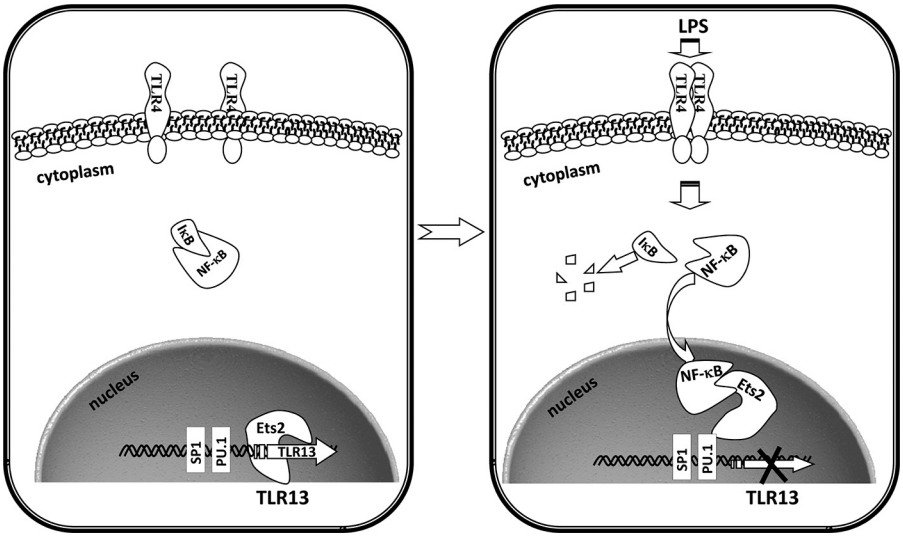

FIGURE 8. **A model of *Tlr13* transcriptional regulation.** *Tlr13* gene transcription is regulated through three *cis*-acting elements that interact with the Ets2, Sp1, and PU.1 transcription factors. In contrast, NF-κB appears to act as an inhibitor of *Tlr13* transcription. The activated signaling of LPS/TLR4 and PGN/TLR2 strongly inhibit the *Tlr13* gene promoter activity, perhaps through NF-κB activation. The inhibition is most likely through p65, which directly interacts with Ets2.

expression of many genes and is frequently localized at the proximal promoter regions as an enhancer (34, 35). Sp1 is a transcription factor containing a zinc finger motif that binds directly to DNA and enhances gene transcription. It is generally believed that Sp1 is part of the basal transcription initiation machinery, particularly for the promoter without a typical TATA box. Because the *Tlr13* promoter lacks a TATA box, Sp1 may function as a linkage with the transcriptional complex. Indeed, we demonstrated that mutation of the Sp1 site dramatically reduced the transcription of *Tlr13* by 75% at the basal level. Sp1 has been reported to mediate the induction of several genes, including human and murine *Tlr2* (36, 37). We show herein that Sp1 alone is necessary but not sufficient for maximal transcriptional activity of *Tlr13*.

To explore the function of *Tlr13* in the innate immune response to infection, we stimulated cells with microbial agents that potentially have the capacity of inducing *Tlr13* expression and activating its specific signaling pathway. However, our data showed that *Tlr13* expression is down-regulated by different microbial stimuli.

The machinery that controls the activation of TLR signaling is complex (38). Known strategies for controlling TLRs signaling include receptor down-regulation, sequestration of Toll-IL-1 receptor adaptors, TRAF6 deubiquitination, and NF-κB degradation (39). However, a simple way in which the immune system could accomplish this regulation might be to tightly control the expression of the TLRs themselves. TLR overexpression is, in fact, detected in various inflammatory diseases. For example, *in vivo* expression of *TLR2* and *TLR4* has been shown to be modulated in patients with rheumatoid arthritis, chronic obstructive pulmonary disease, and sepsis (40–42).

NF-κB is known to regulate the expression of many genes (43), including TLRs. Previous work has demonstrated that NF-κB up-regulates the transcriptional expression of human and mouse *TLR2* (44–46). In contrast, NF-κB down-regulates the transcriptional expression of *TLR9* gene (33). How does NF-κB up-regulate or down-regulate different TLR expression? The mechanism underlying this distinct role of NF-κB is not understood. One possibility is that NF-κB might cooperate with other transcription factors, such as Ets2. Ets2 can up-regulate *Tlr13* through direct binding; however, NF-κB p65 inhibits binding of Ets2 and its ability to activate TLR13 transcriptional activity.

Although the exact role of TLR13 is currently unknown, phylogenic analysis indicates that *Tlr13* is a member of the *Tlr11* subfamily (14). We have previously demonstrated that TLR11 recognizes urinary pathogenic *E. coli* (15). Therefore, to generate more information concerning the possible role of *Tlr13*, we tested bacterial components, including LPS, PGN, and whole bacterial lysates, for their ability to influence *Tlr13* promoter activity. Our work indicates that these components significantly inhibit *Tlr13* promoter activity. In contrast, viral components, such as poly(I-C), do not severely alter *Tlr13* promoter activity, whereas IFN-β slightly increased *Tlr13* promoter activity in our tested fragment. Actually, one possible clue concerning the role of *Tlr13* might be found in recent work generated by the Beutler laboratory (47) and the Ploegh laboratory (48). They claim that *Tlr13*, like *TLR3* and *TLR9*, colocalizes and interacts with UNC93B1, a molecule located in the endoplasmic reticulum (47, 48), and strongly suggest that *Tlr13* might be found inside cells. Our current knowledge about TLR biology indicates that all of the intracellular TLRs, including TLR3, -7, -8, and -9, are nucleic acid sensors and are mainly involved in the recognition of viral infections (3). Therefore, *Tlr13* may also play a similar role in recognizing viral infections. Our multiple tissue Northern blot demonstrated that *Tlr13* is mainly expressed in murine spleen; quantitative real time RT-PCR revealed that *Tlr13* is highly expressed in plasmacytoid dendritic cells,[3] indicating that *Tlr13* might play a role in innate immune responses to virus to activate type I interferon. Thus, *Tlr11* and *Tlr13* seem quite different from each other. *Tlr11* recognizes bacteria, whereas *Tlr13* might recognize virus. However, we have not yet identified the responsible elements, such as interferon regulatory factors, to regulate *Tlr13* promoter activity in response to virus. A further analysis of the upstream regions in the *Tlr13* promoter may reveal elements that control *Tlr13* transcription activity upon viral infection.

In summary, we identified three cis-acting elements, Ets2, PU.1, and Sp1 sites, which play a critical role culminating in the maximal transcriptional activity of *Tlr13*. NF-κB acted as a suppressor. Overexpression of Ets2 potently *trans*-activated the *Tlr13* gene promoter. INF-β is capable of acting TLR13 tran-

[3] Z. Shi and D. Zhang, unpublished data.

scription, but the activated signaling of LPS/TLR4 and PGN/TLR2 strongly inhibited the *Tlr13* gene promoter, perhaps through NF-κB. NF-κB p65 acts an inhibitor in cooperation with *Tlr13 trans*-activator Ets2 (Fig. 8). This work may provide a strong foundation in the function of *Tlr13*, a novel Toll-like receptor in the innate immune response to microbial infection.

Acknowledgment—We thank Lida Keene for critical review of the manuscript.

REFERENCES

1. Janeway, C. A., Jr., and Medzhitov, R. (2002) *Annu. Rev. Immunol.* **20,** 197–216
2. Aderem, A., and Ulevitch, R. J. (2000) *Nature* **406,** 782–787
3. Akira, S., Uematsu, S., and Takeuchi, O. (2006) *Cell* **124,** 783–801
4. Beutler, B. (2002) *Curr. Opin. Hematol.* **9,** 2–10
5. Underhill, D. M., and Ozinsky, A. (2002) *Curr. Opin. Immunol.* **14,** 103–110
6. Lien, E., Means, T. K., Heine, H., Yoshimura, A., Kusumoto, S., Fukase, K., Fenton, M. J., Oikawa, M., Qureshi, N., Monks, B., Finberg, R. W., Ingalls, R. R., and Golenbock, D. T. (2000) *J. Clin. Investig.* **105,** 497–504
7. Janeway, C. A., Jr. (1989) *Cold Spring Harbor Symp. Quant. Biol.* **54**, 1–13
8. Medzhitov, R., and Janeway, C. A., Jr. (1997) *Curr. Opin. Immunol.* **9,** 4–9
9. Janeway, C. A., Jr., and Medzhitov, R. (1999) *Curr. Biol.* **9,** R879–R882
10. Anderson, K. V. (2000) *Curr. Opin. Immunol.* **12,** 13–19
11. Medzhitov, R. (2001) *Nat. Rev. Immunol.* **1,** 135–145
12. Kawai, T., and Akira, S. (2006) *Cell Death Differ.* **13,** 816–825
13. Tabeta, K., Georgel, P., Janssen, E., Du, X., Hoebe, K., Crozat, K., Mudd, S., Shamel, L., Sovath, S., Goode, J., Alexopoulou, L., Flavell, R. A., and Beutler, B. (2004) *Proc. Natl. Acad. Sci. U.S.A.* **101,** 3516–3521
14. Roach, J. C., Glusman, G., Rowen, L., Kaur, A., Purcell, M. K., Smith, K. D., Hood, L. E., and Aderem, A. (2005) *Proc. Natl. Acad. Sci. U.S.A.* **102,** 9577–9582
15. Zhang, D., Zhang, G., Hayden, M. S., Greenblatt, M. B., Bussey, C., Flavell, R. A., and Ghosh, S. (2004) *Science* **303,** 1522–1526
16. Yarovinsky, F., Zhang, D., Andersen, J. F., Bannenberg, G. L., Serhan, C. N., Hayden, M. S., Hieny, S., Sutterwala, F. S., Flavell, R. A., Ghosh, S., and Sher, A. (2005) *Science* **308,** 1626–1629
17. Zhang, D., Cao, D., Russell, R., and Pizzorno, G. (2001) *Cancer Res.* **61,** 6899–6905
18. Rehli, M., Poltorak, A., Schwarzfischer, L., Krause, S. W., Andreesen, R., and Beutler, B. (2000) *J. Biol. Chem.* **275,** 9773–9781
19. Cartharius, K., Frech, K., Grote, K., Klocke, B., Haltmeier, M., Klingenhoff, A., Frisch, M., Bayerlein, M., and Werner, T. (2005) *Bioinformatics* **21,** 2933–2942
20. Chang, F., Steelman, L. S., Lee, J. T., Shelton, J. G., Navolanic, P. M., Blalock, W. L., Franklin, R. A., and McCubrey, J. A. (2003) *Leukemia* **17,** 1263–1293
21. Sharrocks, A. D. (2001) *Nat. Rev. Mol. Cell Biol.* **2,** 827–837
22. Zaldumbide, A., Carlotti, F., Pognonec, P., and Boulukos, K. E. (2002) *J. Immunol.* **169,** 4873–4881
23. Galang, C. K., García-Ramírez, J., Solski, P. A., Westwick, J. K., Der, C. J., Neznanov, N. N., Oshima, R. G., and Hauser, C. A. (1996) *J. Biol. Chem.* **271,** 7992–7998
24. Wei, G., Guo, J., Doseff, A. I., Kusewitt, D. F., Man, A. K., Oshima, R. G., and Ostrowski, M. C. (2004) *J. Immunol.* **173,** 1374–1379
25. Blumenthal, S. G., Aichele, G., Wirth, T., Czernilofsky, A. P., Nordheim, A., and Dittmer, J. (1999) *J. Biol. Chem.* **274,** 12910–12916
26. Rees, L. E., Wood, N. A., Gillespie, K. M., Lai, K. N., Gaston, K., and Mathieson, P. W. (2002) *Cell Mol. Life Sci.* **59,** 560–569
27. Ma, X., Gri, G., and Trinchieri, G. (1996) *Ann. N.Y. Acad. Sci.* **795,** 357–360
28. Gri, G., Savio, D., Trinchieri, G., and Ma, X. (1998) *J. Biol. Chem.* **273,** 6431–6438
29. Jin, D. I., Jameson, S. B., Reddy, M. A., Schenkman, D., and Ostrowski, M. C. (1995) *Mol. Cell. Biol.* **15,** 693–703
30. Sevilla, L., Zaldumbide, A., Carlotti, F., Dayem, M. A., Pognonec, P., and Boulukos, K. E. (2001) *J. Biol. Chem.* **276,** 17800–17807
31. Moulton, K. S., Semple, K., Wu, H., and Glass, C. K. (1994) *Mol. Cell. Biol.* **14,** 4408–4418
32. Shibata, Y., Berclaz, P. Y., Chroneos, Z. C., Yoshida, M., Whitsett, J. A., and Trapnell, B. C. (2001) *Immunity* **15,** 557–567
33. Takeshita, F., Suzuki, K., Sasaki, S., Ishii, N., Klinman, D. M., and Ishii, K. J. (2004) *J. Immunol.* **173,** 2552–2561
34. Courey, A. J., Holtzman, D. A., Jackson, S. P., and Tjian, R. (1989) *Cell* **59,** 827–836
35. Bouwman, P., and Philipsen, S. (2002) *Mol. Cell. Endocrinol.* **195,** 27–38
36. Medzhitov, R., Preston-Hurlburt, P., and Janeway, C. A., Jr. (1997) *Nature* **388,** 394–397
37. Tötemeyer, S., Foster, N., Kaiser, P., Maskell, D. J., and Bryant, C. E. (2003) *Infect. Immun.* **71,** 6653–6657
38. Liew, F. Y., Xu, D., Brint, E. K., and O'Neill, L. A. (2005) *Nat. Rev. Immunol.* **5,** 446–458
39. Bowie, A. G. (2008) *Nat. Immunol.* **9,** 348–350
40. Iwahashi, M., Yamamura, M., Aita, T., Okamoto, A., Ueno, A., Ogawa, N., Akashi, S., Miyake, K., Godowski, P. J., and Makino, H. (2004) *Arthritis Rheum.* **50,** 1457–1467
41. Andreakos, E., Foxwell, B., and Feldmann, M. (2004) *Immunol. Rev.* **202,** 250–265
42. Armstrong, L., Medford, A. R., Hunter, K. J., Uppington, K. M., and Millar, A. B. (2004) *Clin. Exp. Immunol.* **136,** 312–319
43. Hayden, M. S., and Ghosh, S. (2008) *Cell* **132,** 344–362
44. Johnson, C. M., and Tapping, R. I. (2007) *J. Biol. Chem.* **282,** 31197–31205
45. Haehnel, V., Schwarzfischer, L., Fenton, M. J., and Rehli, M. (2002) *J. Immunol.* **168,** 5629–5637
46. Wang, T., Lafuse, W. P., and Zwilling, B. S. (2001) *J. Immunol.* **167,** 6924–6932
47. Tabeta, K., Hoebe, K., Janssen, E. M., Du, X., Georgel, P., Crozat, K., Mudd, S., Mann, N., Sovath, S., Goode, J., Shamel, L., Herskovits, A. A., Portnoy, D. A., Cooke, M., Tarantino, L. M., Wiltshire, T., Steinberg, B. E., Grinstein, S., and Beutler, B. (2006) *Nat. Immunol.* **7,** 156–164
48. Kim, Y. M., Brinkmann, M. M., Paquet, M. E., and Ploegh, H. L. (2008) *Nature* **452,** 234–238